



ChemComm

**Photostability of luminescent  
tris(2,4,6-trichlorophenyl)methyl radical enhanced by  
terminal modification of carbazole donor**

Journal:	<i>ChemComm</i>
Manuscript ID	CC-COM-08-2022-004481.R2
Article Type:	Communication

SCHOLARONE™  
Manuscripts

## COMMUNICATION

Photostability of luminescent *tris*(2,4,6-trichlorophenyl)methyl radical enhanced by terminal modification of carbazole donor

Received 00th January 20xx,  
Accepted 00th January 20xx

Kenshiro Matsuda,<sup>a</sup> Rui Xiaotian,<sup>a</sup> Kazuhiro Nakamura,<sup>a</sup> Minori Furukori,<sup>b, c</sup> Takuya Hosokai,<sup>\*b, c</sup> Kosuke Anraku,<sup>a</sup> Kohei Nakao,<sup>d</sup> and Ken Albrecht<sup>\*d, e</sup>

DOI: 10.1039/x0xx00000x

**Stable organic luminescent radicals have attracted much attention, but their stability under light irradiation is not yet satisfactory. New luminescent radicals (TTMs) based on terminal benzene ring modified carbazole donors were synthesized and evaluated. Their photostability (half-life under continuous laser irradiation) has improved by 1 order of magnitude compared to simple carbazole donors. This is a new molecular design strategy to improve the photostability of luminescent radicals without reducing other photophysical properties.**

Stable organic luminescent radicals have attracted much attention due to their optical and magneto-optical properties.<sup>1, 2, 3, 4, 5, 6, 7</sup> TTM (tris-2,4,6-trichlorophenylmethyl)<sup>8</sup> and PTM<sup>9</sup> (perchloro triphenylmethyl) radicals are typical stable luminescent radical species due to the steric protection by bulky chlorine atoms and spin delocalization over the aromatic rings (Fig. 1). Their stability in dark ambient conditions is high enough to handle, but the stability under photoexcitation conditions is known to be poor.<sup>8</sup> The introduction of a donor molecule<sup>10</sup> or replacing the benzene ring with pyridine<sup>11, 12, 13, 14</sup> has been reported to improve photostability dramatically. The carbazole (Cz) donor is frequently used to stabilize the excited state and boost the photoluminescence quantum yield (PLQY) due to the excited state charge transfer character.<sup>15</sup> Several Cz moieties have been attached to TTM radicals with different substitution patterns,<sup>16, 17</sup> but the structure-stability relationship and strategy to improve the photostability are not sufficiently established.<sup>18</sup>

Carbazole is a classic heterocyclic compound that is widely studied as photonic and electronic material largely owing to the donor character.<sup>19, 20, 21, 22, 23</sup> Due to the intrinsic hole-transporting property and luminescent properties, Cz is a promising building block for organic light-emitting diode (OLED) materials.<sup>24</sup> Most simple Cz attached to luminescent TTM radical [4-(N-carbazolyl)-2,6-dichlorophenyl]bis(2,4,6-trichlorophenyl) methyl; Cz-TTM) has been first reported in 2006<sup>10</sup> and applied as emitting material in OLEDs in 2015.<sup>25</sup> Cz-TTM has a doublet character both in the

ground state and excited state, which theoretically allows 100% exciton utilization efficiency in OLED devices.<sup>26</sup> This is in contrast with usual ground state singlet molecules because the excitons formed in OLED devices will be singlet and triplet excited states, and a spin-flipping process is required to achieve 100% exciton utilization efficiency. When the 6-5-6 fused ring structure such as Cz is attached to TTM, the symmetry will be broken, which can boost the PLQY of TTM radical.<sup>16</sup> Donor substitution also improves photostability, but the photostability and stability under device operating conditions are still insufficient.

Enhancing the photostability of TTM and establishing the molecular design strategy are critical tasks for organic radicals. Although the photostability changes with the chemical structure and electronic structure,<sup>18</sup> no studies focus on modifying the Cz donor itself. Cz cation radicals are unstable and well known to undergo dimerization at the 3,6,9- position,<sup>27, 28, 29</sup> and blocking this position is effective in improving the stability. Here we report the photophysical influence of modifying the terminal of Cz unit of Cz-TTM. The new Cz stabilization strategy is simple but effective in improving the photostability of luminescent radicals (Fig. 1).

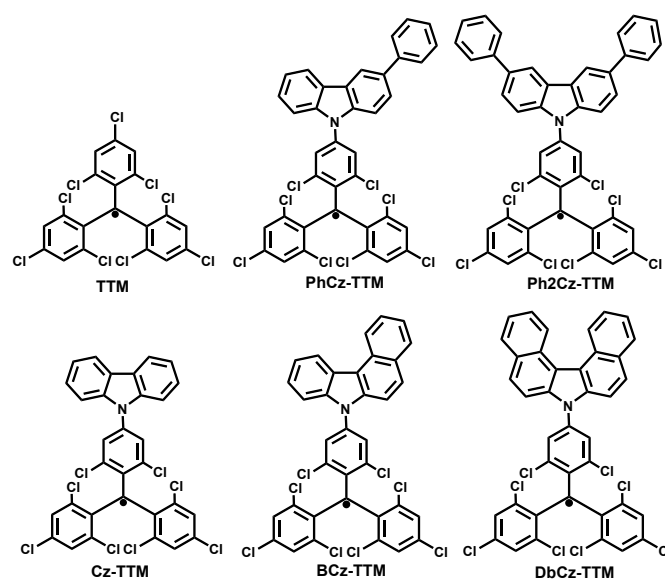


Fig. 1 Structure of terminal modified carbazole-TTM radicals.

The Cz-substituted TTM radicals were synthesized using a similar procedure as previously reported, i.e., the nucleophilic aromatic

<sup>a</sup> Interdisciplinary Graduate School of Engineering Sciences, Kyushu University, 6-1 Kasuga-Koen Kasuga-shi Fukuoka 816-8580, Japan.

<sup>b</sup> Department of Pure and Applied Chemistry, Faculty of Science and Technology, Tokyo University of Science, 2641 Yamazaki, Noda, Chiba 278-8510, Japan.

<sup>c</sup> National Institute of Advanced Industrial Science and Technology (AIST), Tsukuba Central 5, 1-1-1 Higashi, Tsukuba, Ibaraki 305-8565, Japan. E-mail: t.hosokai@aist.go.jp

<sup>d</sup> Institute for Materials Chemistry and Engineering, Kyushu University, 6-1 Kasuga-Koen Kasuga-shi Fukuoka 816-8580, Japan. E-mail: albrecht@cm.kyushu-u.ac.jp

<sup>e</sup> JST-PRESTO, 4-1-8 Honcho, Kawaguchi, Saitama 332-0012, Japan.

† Electronic Supplementary Information (ESI) available: [details of any supplementary information available should be included here]. See DOI: 10.1039/x0xx00000x

substitution reaction between TTM radical and carbazoles to obtain the radical precursor (HTTM) and following the radicalization process.<sup>10</sup> TTM radical,  $\text{Cs}_2\text{CO}_3$ , and Cz derivatives were heated under a nitrogen atmosphere with DMF as solvent at 160°C for 12h. Radical precursors were purified using preparative scale gel permeation chromatography (GPC). The yields were PhCz-HTTM (30%), Ph2Cz-HTTM (28%), BCz-HTTM (34%) and DbCz-HTTM (30%), respectively. The radical precursors were dissolved in THF, *t*-BuOK was added, and stirred in the dark for 5 h to form an anion. *p*-Chloranil was added and stirred for 3 h at room temperature to form radical through a one-electron oxidation process. The final products were purified by flash silica gel column chromatography (eluent: toluene: hexane=1: 9). The yield was PhCz-TTM (58%), Ph2Cz-TTM (42%), BCz-TTM (55%) and DbCz-TTM (50%), respectively. All precursors were characterized with Mass spectrometry (FAB-MS), <sup>1</sup>H NMR, <sup>13</sup>C NMR, and elemental analysis, and the radicals were characterized with Mass spectrometry (FAB-MS), elemental analysis, and Electron Spin Resonance (ESR) (Fig. S1-9, Scheme S1 ES†).

The radical (TTM) and precursor (HTTM) are difficult to separate, and the purity of the radical cannot be determined by elemental analysis or mass spectroscopy due to the difference of only 1 proton. In previous reports, the purity of the radical was not determined accurately, and for example, the molar excitation coefficient of Cz-TTM is reported to be in the range of 2940 to 3780  $\text{M}^{-1}\text{cm}^{-1}$ .<sup>30, 15</sup> The <sup>1</sup>H NMR measurement of the synthesized radicals revealed that some precursors remain. The actual radical purity was determined by quantifying the content of radical precursors using qNMR. Radical purities were determined to be 83% (Cz-TTM), 99% (PhCz-TTM), 99% (Ph2Cz-TTM), 99% (BCz-TTM) and 99% (DbCz-TTM), respectively by assuming the impurity is only the precursor (HTTMs) (Fig. S10-S14, TableS1). The radical purity was considered in the following discussion to correct the photophysical data.

The UV-vis absorption spectra of radicals were measured in cyclohexane, toluene, and chloroform (Figs. 2, S2, S3, Table S1). UV-vis spectra showed an absorption band attributed to charge transfer (CT) from Cz to TTM at 603 nm (Cz-TTM), 616 nm (PhCz-TTM), 628 nm (Ph2Cz-TTM), 607 nm (BCz-TTM), and 599 nm (DbCz-TTM) in cyclohexane, respectively. Molar absorption coefficients were measured in chloroform and calibrated with the purity of the radicals. The molar absorption coefficients ( $\epsilon$ ) was Cz-TTM 597 nm ( $\epsilon = 3.7 \times 10^3 \text{ M}^{-1}\text{cm}^{-1}$ ), PhCz-TTM 608 nm ( $\epsilon = 2.9 \times 10^3 \text{ M}^{-1}\text{cm}^{-1}$ ), Ph2Cz-TTM 618 nm ( $\epsilon = 3.1 \times 10^3 \text{ M}^{-1}\text{cm}^{-1}$ ), BCz-TTM 596 nm ( $\epsilon = 3.2 \times 10^3 \text{ M}^{-1}\text{cm}^{-1}$ ), and DbCz-TTM 584 nm ( $\epsilon = 2.8 \times 10^3 \text{ M}^{-1}\text{cm}^{-1}$ ), respectively (Fig. S15-S18, Table 1, S2-S3). No significant change in the molar absorption coefficient was observed for all radicals. This absorption band showed solvent polarity dependence, confirming the CT character of the excited state (Fig. 2, Table S2). The charge transfer from the carbazole unit to TTM radical could also be observed by visualizing the molecular orbitals by DFT calculations (Figs. S19-S23). On the other hand, the absorption peak at 374 nm attributed to the local absorption of the TTM moiety was intact to the solvent and structure of Cz moiety (Fig. S15, S16).<sup>15</sup> The absorption of the CT transition had shifted to a longer wavelength when Ph rings were substituted to the 3,6-position because of the extension of  $\pi$ -conjugation of Cz. In the case of Ph ring fusion, the absorption of CT transition was almost intact, or even a slight blue shift was observed in DbCz-TTM compared to Cz-TTM. The DFT calculations show that the HOMO level of Cz increases upon the ring fusion, and this behavior cannot be explained (Figs. S19-S23). The

unexpected behavior may be explained by considering the electronic repulsion energy that is characteristic of radical species.<sup>31,32</sup> The UV-vis absorption revealed that the Cz modification does not influence the electronic state of the TTM, but perturbs the CT transition.

The PL spectra of radicals were measured in cyclohexane and toluene (Fig. 2, S24 Tables 1, S2). The PL spectra was broad and appeared at a longer wavelength in toluene compared to cyclohexane. This behavior is consistent with UV-vis spectra and indicates that the emission is from a CT excited state. The emission maxima in cyclohexane were Cz-TTM (628 nm, 1.97 eV), BCz-TTM (637 nm, 1.95 eV), PhCz-TTM (648 nm, 1.91 eV), and Ph2Cz-TTM (661 nm, 1.88 eV), respectively. The emission of Ph2Cz-TTM was red-shifted by about 30 nm (0.09 eV) compared to unsubstituted Cz-TTM, and the trend was similar to the UV-vis absorption spectra. DbCz-TTM showed exceptional emission spectra, i.e., a second emission band at a longer wavelength appeared. The spectra shape did not change in a concentration range of 100  $\mu\text{M}$  to 0.1  $\mu\text{M}$ , implying that the intermolecular excimer formation was denied. The emission lifetime was the same for both emission peaks. At this point, the origin is unclear, but it can be attributed to the vibronic structure or the helicene-like structure of DbCz moiety that may form an intramolecular excimer-like structure. Time-resolved PL and/or transient absorption spectroscopy may give a hint to reveal the origin of the peculiar PL spectra of DbCz-TTM.

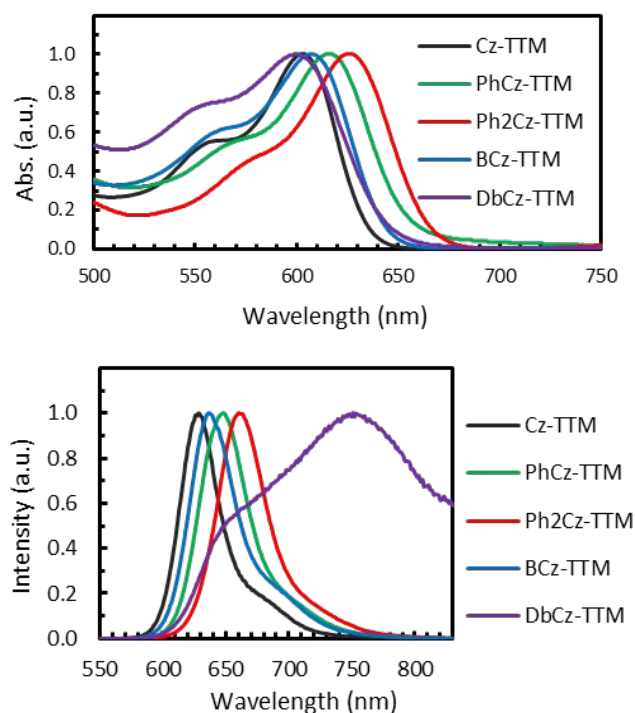


Fig. 2 (top) UV-vis and (down) PL spectra of terminal modified carbazole-TTM radicals in cyclohexane.

PL lifetime and PLQY of TTM derivatives were measured, and the rate constants were determined in cyclohexane and toluene (Figs. S25-S31, Tables 1, S2). The PL lifetimes in cyclohexane were 41.7 ns (Cz-TTM), 34.5 ns (PhCz-TTM), 32.3 ns (Ph2Cz-TTM), 37 ns (BCz-TTM), and 25 ns (DbCz-TTM), respectively. PLQY in cyclohexane

Table 1 Photophysical properties of radicals in cyclohexane

Compounds	$\lambda_{\text{Abs}}(\text{nm})^{\text{a}}$	$\lambda_{\text{PL}}(\text{nm})^{\text{a}}$	$\lambda_{\text{a}}-\lambda_{\text{PL}}(\text{cm}^{-1})$	$t_{1/2}(10^3 \text{ s})^{\text{b}}$	PLQY (%) <sup>b</sup>	$\tau(\text{ns})^{\text{b}}$	$k_{\text{f}}(10^6 \text{ s}^{-1})$	$k_{\text{nr}}(10^6 \text{ s}^{-1})$	$\epsilon(10^3 \text{ M}^{-1} \text{ cm}^{-1})^{\text{c}}$
Cz-TTM	603	628	660	2.40	78	41.7	19	5.4	3.7
PhCz-TTM	616	648	802	25.5	62	34.5	18	11	2.9
Ph2Cz-TTM	628	661	795	47.2	69	32.3	22	9.5	3.1
BCz-TTM	607	637	776	11.9	61	37.0	17	10	3.2
DbCz-TTM	599	650/751	1310	60.8	3	25.0	1.2	39	2.8

a) Absorption ( $\lambda_{\text{Abs}}$ ), PL ( $\lambda_{\text{PL}}$ ) were measured in cyclohexane solutions (ca.  $10^{-5}$  M), b)  $t_{1/2}$ ,  $\tau$  and PLQY were measured absorbance of 0.5[-] at 355 nm in cyclohexane and calibrated for radical purity, c) The molar absorption coefficient was measured in chloroform according to Lambert-Beer's law and calibrated by the purity of the radicals (Fig. S4).

was 78% (Cz-TTM), 62% (PhCz-TTM), 69% (Ph2Cz-TTM), 61% (BCz-TTM), and 3% (DbCz-TTM), respectively. From the PLQY and PL lifetime, the rate constants for radiative ( $k_{\text{f}}$ ) and non-radiative deactivation ( $k_{\text{nr}}$ ) were determined. The rate constants of all compounds are similar except DbCz-TTM (Table 1). DbCz-TTM has a smaller  $k_{\text{f}}$  and larger  $k_{\text{nr}}$  compared to other compounds. The reason for the increase of  $k_{\text{nr}}$  is unclear, but the helicene-like structure may cause the flipping motion, and the intramolecular excimer-like structure may cause a larger thermal deactivation path. Actually, this is constant with literature that reports DbCz modified CT molecule had low PLQY compared to other substituents.<sup>33</sup> It was shown that neither the attachment of a Ph ring to Cz nor the fusion of a Ph ring had a significant effect on PLQY in compounds except for DbCz-TTM.

The unrestricted Kohn-Sham density functional theory (UKS-DFT) calculations using Gaussian 16 with UB3LYP functional and 6-31G\*\* basis sets were performed in a vacuum to understand the electronic structure.<sup>34</sup> The HOMO-SOMO energies were obtained to give an orbital description of the lowest energy absorption band. The energy difference between HOMO and SOMO as 2.35 eV (Cz-TTM, 172b-171b), 2.20 eV (PhCz-TTM, 192b-191b) and 2.12 eV (Ph2Cz-TTM, 212b-211b), 2.11 eV (BCz-TTM, 212b-211b), and 1.87 eV (DbCz-TTM, 198b-197b), respectively (Figs. S19-S23). Calculations show that the lowest absorption band is likely the CT absorption from the Cz derivative to TTM. As mentioned in the UV-vis absorption section, calculations show that the HOMO level of Cz increases upon the ring fusion, and the trend of the bandgap was consistent with Ph substituted compounds. However, the behavior of ring fusion could not be explained probably because the electronic repulsion energy is not considered in the calculation.<sup>31</sup> The energy levels of DbCz-TTM showed an inversion of HOMO-SOMO, which is called a non-Aufbau electronic structure.<sup>18, 35</sup> However, note that this result can depend on the calculation level.

Cyclic voltammetry (CV) was measured to determine the redox potential and effect of Cz moieties (Fig. S32). All radicals showed a reversible redox reaction similar to TTM. The reduction/oxidation potentials were -1.14/0.87 V vs  $\text{FC}^+/\text{FC}$  (TTM), -1.09/0.58 V vs  $\text{FC}^+/\text{FC}$  (Cz-TTM), -1.10/0.56 V vs  $\text{FC}^+/\text{FC}$  (PhCz-TTM), -1.07/0.53 V vs  $\text{FC}^+/\text{FC}$  (Ph2Cz-TTM), -1.11/0.62 V vs  $\text{FC}^+/\text{FC}$  (BCz-TTM), and -1.12/0.69 V vs  $\text{FC}^+/\text{FC}$  (DbCz-TTM), respectively. The first redox is attributed to the reduction of TTM radical (SOMO), and the potential did not change significantly.<sup>36, 37</sup> This result is consistent with the UV-vis spectra, i.e., the electronic structure of the TTM radical itself does not change when Cz moieties are substituted. On the other hand, the oxidation peak shifted to a lower potential when Cz moieties were substituted with TTM. This can be explained by the quinoid-type resonance structure of the cation radical species.<sup>38</sup> The trend of the gap

between two redox potentials has well matched the trend of UV-vis absorption of the CT band (smaller energy upon Ph ring substitution and larger energy upon Ph ring fusion). The CV measurement indicates that the SOMO of TTM moiety is not affected by the Cz moiety, but the HOMO level is affected through the conjugated electronic communication of the Cz and TTM moiety.

The photostability of each radical was observed by monitoring the PL intensity during continuous irradiation with a 355 nm pulsed laser in cyclohexane, and the half-life values were calibrated according to the purity and absorption coefficient of the radicals and precursor at 355 nm (Fig. 3, S33, Table S2-S4). Note that the absorbance of all compounds was controlled to be 0.5 at 355 nm, and the solutions were stirred during the measurement without degassing (Fig. S2). Under the same conditions, the half-life of bare TTM radical was shown to be  $4.77 \times 10^1 \text{ s}$ . The half-life of Cz attached radicals was much improved to be  $2.40 \times 10^3 \text{ s}$  (Cz-TTM),  $2.55 \times 10^4 \text{ s}$  (PhCz-TTM),  $4.72 \times 10^4 \text{ s}$  (Ph2Cz-TTM),  $1.19 \times 10^4 \text{ s}$  (BCz-TTM), and  $6.08 \times 10^4 \text{ s}$  (DbCz-TTM), respectively. Compared to Cz-TTM, the Ph ring substitution and Ph ring fusion improved the photostability 1 order of magnitude. The reason for the large increase is unclear, but the stabilization of the cation radical of carbazole in the excited state by larger conjugation and blocking the 3,6-position can be a possible explanation.<sup>37</sup> The photostability of Cz TTM can be enhanced more than 1 order of magnitude by Ph ring substitution and fusion.

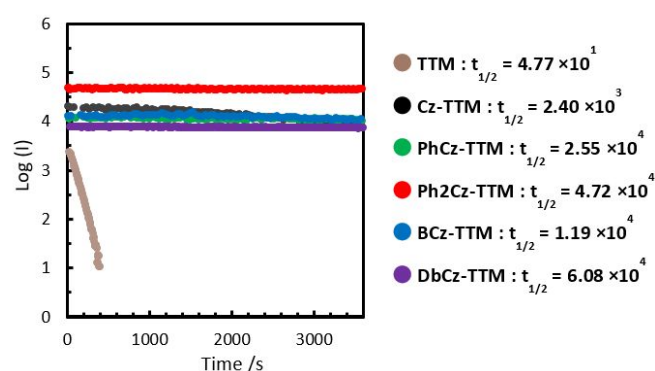


Fig. 3 Time dependence of the emission intensity ( $I$ ) for radicals in cyclohexane under 355 nm pulsed laser radiation (power: 0.7 mW, beam diameter ( $1/e^2$  level):  $\sim 3$  mm, pulse width: 28 ps, repetition rate: 10 Hz). Intensity ( $I$ ) depends on the detector position and the absolute value does not reflect the physical property such as PLQY.

In conclusion, the effect of terminal Ph ring modification of Cz-TTM luminescent radicals was investigated. Ph substitution resulted in a shift of absorption and emission towards longer wavelengths and a minimal decrease in PLQY. Ring fusion of benzene to Cz did not affect absorption and emission wavelengths as much as Ph substitution, but the PLQY of DbCz-TTM was reduced compared to the other compounds. The photostability of all compounds was 1 orders of magnitude greater than that of Cz-TTM. This indicates that not only the TTM structure but also the donor structure has a strong influence on the stability of the luminescent radicals. This study shows a simple method for improving the stability of luminescent radicals without diminishing luminescent property. Research on OLED devices is underway, and this molecular design is expected to improve the device performance.

This work was supported, in part, by JSPS KAKENHI Grant Nos. JP18H03902, JP20H02801, JP21H05399, and "Dynamic Alliance for Open Innovation Bridging Human, Environment and Materials", and Leading Initiative for Excellent Young Researchers, Grant-in-Aid for "2019 Initiative for Realizing Diversity in the Research Environment" through the "Diversity and Super Global Training Program for Female and Young Faculty (SENTAN-Q)", Kyushu University from MEXT. JST PRESTO Grant Number JPMJPR18T2. This study was also supported by the AIST Nanocharacterization Facility (ANCF) platform as a program of the "Nanotechnology Platform" of the Ministry of Education, Culture, Sports, Science, and Technology (MEXT), Japan (Grant Number JPMXP09A21AT0017). KM, RX and KA want to thank Ms. Keiko Idea for helping NMR and ESR measurements.

### Conflicts of interest

There are no conflicts to declare.

### Notes and references

- 1 S. Kimura, K. Kato, Y. Teki, H. Nishihara and T. Kusamoto, *Chem. Sci.*, 2021, **12**, 2025–2029.
- 2 S. Kimura, M. Uejima, W. Ota, T. Sato, S. Kusaka, R. Matsuda, H. Nishihara, and T. Kusamoto *J. Am. Chem. Soc.* 2021, **143**, 4329–4338
- 3 X. Ai, Y. Chen, Y. Feng, and F. Li, *Angew. Chem. Int. Ed.*, 2018, **57**, 2869–2873.
- 4 Z. X. Chen, Y. Li and F. Huang, *Chem*, 2021, **7**, 288–332.
- 5 A. Abdurahman, Q. Peng, O. Ablikim, X. Ai and F. Li, *Mater. Horiz.* 2019, **6**, 1265–1270.
- 6 H. Namai, H. Ikeda, Y. Hoshi, N. Kato, Y. Morishita, and K. Mizuno, *J. Am. Chem. Soc.* 2007, **129**, 9032–9036.
- 7 Liu, C. H. Hamzehpoor, E. Sakai-Otsuka, Y. Jadhav, T. Perepichka, D. F., *Angew. Chem., Int. Ed.* 2020, **59**, 23030–23034.
- 8 O. Armet, J. Veciana, C. Rovira, J. Riera, J. Castaner, E. Molins, J. Rius, C. Miravittles, S. Olivella and J. Brichfeus, *J. Phys. Chem.*, 1987, **91**, 5608–5616.
- 9 M. Ballester, J. Riera-Figueras and A. Rodríguez-Siurana, *Tetrahedron Lett.*, 1970, **11**, 3615–3618.
- 10 V. Gamerao, D. Velasco, S. Latorre, F. López-Calahorra, E. Brillasc and L. Juliá, *Tetrahedron Lett.*, 2006, **47**, 2305–2309.
- 11 Y. Hattori, T. Kusamoto and H. Nishihara, *Angew. Chem. Int. Ed.*, 2014, **44**, 11845–11848.
- 12 Y. Hattori, T. Kusamoto and H. Nishihara, *Angew. Chem., Int. Ed.*, 2015, **54**, 3731–3734
- 13 Y. Hattori, T. Kusamoto, T. Sato and H. Nishihara, *Chem. Commun.*, 2016, **52**, 13393–13396.
- 14 S. Kimura, A. Tanushi, T. Kusamoto, S. Kochi, T. Sato and H. Nishihara, *Chem. Sci.*, 2018, **9**, 1996–2007
- 15 A. Abdurahman, T. J. H. Hele, Q. Gu, J. Zhang, Q. Peng, M. Zhang, R. H. Friend, F. Li and E. W. Evans, *Nat. Mater.*, 2020, **19**, 1224–1229.
- 16 X. Ai, E. W. Evans, S. Dong, A. J. Gillett, H. Guo, Y. Chen, T. J. H. Hele, R. H. Friend and F. Li, *Nature*, 2018, **563**, 536–540.
- 17 L. Chen, M. Arnold, Y. Kittel, R. Blinder, and F. Jelezko, A. J. C. Kuehne, *Adv. Opt. Mater.* 2022, **10**, 2102101
- 18 H. Guo, Q. Peng, X. Chen, Q. Gu, S. Dong, E. W. Evans, A. J. Gillett, X. Ai, M. Zhang, D. Credginton, V. Coropceanu, R. H. Friend, J. Brédas and F. Li, *Nat. Mater.*, 2019, **18**, 977–984.
- 19 J.V. Grazulevicius, P. Strohrriegl, J. Pielichowski and K. Pielichowski, *Prog. Polym. Sci.*, 2003, **28**, 1297–1353.
- 20 H. Uoyama, K. Goushi, K. Shizu, H. Nomura and C. Adachi, *Nature*, 2012, **492**, 234–238.
- 21 K. Albrecht and K. Yamamoto, *J. Am. Chem. Soc.*, 2009, **131**, 2244–2251.
- 22 K. R. J. Thomas, J. T. Lin, Y. Tao, and C. Ko, *J. Am. Chem. Soc.* 2001, **123**, 38, 9404–9411
- 23 K. Albrecht, K. Matsuoka, K. Fujita, and K. Yamamoto, *Angew. Chem. Int. Ed.*, 2015, **54**, 5677–5682.
- 24 Y. Shiota and H. Kageyama, *Chem. Rev.*, 2007, **107**, 953–1010.
- 25 Q. Peng, A. Obolda, M. Zhang, and F. Li, *Angew. Chem. Int. Ed.*, 2015, **54**, 7091–7095.
- 26 A. Obolda, X. Ai, M. Zhang, and F. Li, *ACS Appl. Mater. Interfaces*. 2016, **8**, 35472–35478.
- 27 J. F. Ambrose and R. F. Nelson, *J. Electrochem. Soc.*, 1968, **115**, 1159.
- 28 K. Karon and M. Lapkowski, *J Solid State Electrochem.*, 2015, **19**, 2601–2610.
- 29 K. Albrecht, R. Pernites, M. J. Felipe, R. C. Advincula, and K. Yamamoto, *Macromolecules*, 2012, **45**, 3, 1288–1295.
- 30 S. Castellanos, D. Velasco, F. Lopez-Calahorra, Enric Brillas, and L. Julia, *J. Org. Chem.* 2008, **73**, 3759–3767
- 31 H. J. Kulik, *J. Chem. Phys.*, 2015, **142**, 240901.
- 32 S. M. Rivero, R. Shang, H. Hamada, Q. Yan, H. Tsuji, E. Nakamura, and J. Casado, *Bull. Chem. Soc. Jpn.*, 2021, **94**, 989–996.
- 33 K. Albrecht, K. Matsuoka, D. Yokoyama, Y. Sakai, A. Nakayama, K. Fujita and K. Yamamoto, *Chem. Commun.*, 2017, **53**, 2439–2442.
- 34 Gaussian 16, Revision B.01, M. J. Frisch. *et al.* Gaussian, Inc., Wallingford CT (2016).
- 35 Sitthichok Kasemthaveechok, Laura Abella, Marion Jean, Marie Cordier, Thierry Roisnel, Nicolas Vanthuyne, Thierry Guizouarn, Olivier Cador, Jochen Autschbach, Jeanne Crassous, and Ludovic Favereau *J. Am. Chem. Soc.* 2020, **142**, 20409–20418.
- 36 A. Tanushi, S. Kimura, T. Kusamoto, M. Tominaga, Y. Kitagawa, M. Nakano, and H. Nishihara, *J. Phys. Chem. C* 2019, **123**, 4417–4423.
- 37 C. Yan, D. An, W. Chen, N. Zhang, Y. Qiao, J. Fang, X. Lu, G. Zhou and Y. Liu, *CCS Chem.*, 2022, **4**, 3190–3203.
- 38 A. Bobet, A. Cuadrado, L. Fajará, I. Sirés, E. Brillas, M. P. Almajano, V. Jankauskas, D. Velasco and L. Juliá, *J. Phys. Org. Chem.*, 2019, **32**, e3974.